JOURNAL OF MATERIALS SCIENCE 22 (1987) 2833–2841

Adhesion to skin

Part 2 *Measurement of interfacial energies for pressure sensitive adhesives*

E. H. ANDREWS, T. A. KHAN, N. A. LOCKINGTON
Materials Department, Queen Mary College, Mile End Road, London E1 4NS, UK

The failure energy of an adhesive bond can be factorized into two terms, one of which is a dimensionless loss function and the other, the true interfacial bonding energy, θ_0. Experimental techniques have been developed to effect a separation of these two terms and thus measure θ_0, but they are unsuitable for the pressure-sensitive adhesives used in surgical tapes and dressings. This is because these adhesives flow readily under load. This paper describes an extrapolation technique by which this problem can be resolved. Adhesive peel data are extrapolated both to zero peel velocity and zero load, to give a true threshold value for peeling energy which is independent of temperature. Values of θ_0 are given for a natural-rubber based adhesive and substrates of glass and human skin *in vivo*. For glass $\theta_0 = 28\,J\,m^{-2}$ and for normal skin $\theta_0 \simeq 14\,J\,m^{-2}$.

1. Introduction

This paper is one of a series concerned with the adhesion of surgical pressure-sensitive adhesive tapes to human skin. The first paper described a novel "soft machine" peel test [1], while Part 3 [2] investigates the effects of absorbed sebum on the adhesive properties. In this paper we evaluate the interfacial energy between adhesive and skin. It was first proposed by Gent and Schultz [3] on the basis of experimental findings, that the adhesive failure energy θ (per unit area of interface) might be expressed as the product of the true interfacial energy θ_0 and a term expressing energy dissipation in the system. This proposal was later confirmed theoretically and experimentally by Andrews and Kinloch [4, 5]. The results obtained can thus be written.

$$\theta = \theta_0 \Phi(\dot{c}, T, \varepsilon_0) \quad (1)$$

where Φ is the "loss function", a dimensionless function depending on rate, $\dot{c}$, temperature, T, and overall strain level, ε_0. The theory of "generalized fracture mechanics" [6] provides the explicit form of Φ in terms of energy-density distribution functions and the hysteresial properties of the system.

Andrews and Kinloch were able to evaluate θ_0 for a cross-linked rubber adhesive bonded to a range of plastic films and showed that θ_0 equalled the calculated thermodynamic work of adhesion, w_A, provided that no primary atomic bonds were created at the interface. Later, Andrews and co-workers [7–9] applied similar methods to the evaluation of θ_0 for epoxy-to-metal and epoxy-to-glass adhesives bonds and followed changes in θ_0 due to the hydrolysis of interfacial atomic bonds.

If the adhesive displays simple visco-elasticity, and the substrate is rigid, the dissipative terms tend to zero at high temperatures and low rates. These conditions can be satisfied using cross-linked gum rubbers as adhesives, and conditions of adhesive separation can be established where $\Phi = 1$. Then the measured adhesive failure energy θ equals θ_0, and this condition is indicated when θ becomes independent of rate at very low rates of debonding. The very low rates of debonding involved are sometimes obtained using fatigue crack propagation.

Taking this approach, Ahagon and Gent [10] measured θ_0 values for styrene–butadiene rubber adhering to glass primed with varying amounts of coupling agent. They obtained values in the range 1.5 to $50\,J\,m^{-2}$. Similarly, Kendall [11] using a smooth rubber sphere contacting a glass plate, measured rate independent θ values of around $0.1\,J\,m^{-2}$.

Turning to pressure-sensitive adhesives, the problem of measuring θ_0 is greatly increased. This is because there is no rate of debonding at which a stressed adhesive joint behaves elastically (i.e. at which dissipation becomes zero and $\Phi \to 1$). Pressure sensitive adhesives are capable of irreversible flow under any finite stress, and measurements of θ at decreasing debonding rate never exhibit a rate-independent region as the rate tends to zero. Instead, at some point, there occurs a transition in the failure mode from adhesive (interfacial failure) to cohesive (bulk failure of the adhesive). This transition clearly arises from the liquid like character of uncrosslinked adhesives which allows them to fail by flow instability provided sufficient time is available. At higher rates of debonding, molecular entanglements impart rubberlike integrity to the adhesive, suppress flow, and thus shift the locus of failure to the adhesive interface.

Adhesive/cohesive failure transitions are one manifestation of the propensity for flow in pressure-sensitive adhesives. Another is the departure of peel testing results from their theoretical behaviour. For a peel test in which the adhesive is supported on a flexible backing which is, at the same

0022–2461/87 $03.00 + .12

time, stiff in tension, the peeling energy θ is given by [12].

$$\theta = \frac{P}{b}(1 - \cos\phi) \equiv F(1 - \cos\phi) \quad (2)$$

where P is the peel force, b the width of the peel strip and ϕ the peeling angle. If, therefore, F or (P/b) is plotted against $(1 - \cos\phi)^{-1}$, a straight line through the origin should be obtained with a slope equal to θ, provided the rate and temperature are the same for all measurements.

A special case of this plot is obtained if the angle ϕ is diminished to the point where adhesive peeling ceases (though cohesive failure may still occur), since then the value of θ given by Equation 2 should be the threshold value, that is, θ_0.

The way in which Equations 1 and 2 can be used to obtain θ_0 values for pressure-sensitive adhesives, which exhibit flow, is the subject of this paper.

2. Outline of method

The basic concept is that, for uncrosslinked adhesives, peel data must be extrapolated both to zero rate *and zero load* to give a true measure of the threshold or intrinsic debonding energy θ_0. Just as extrapolation to zero debonding rate eliminates visco-elastic dissipation terms from θ, so extrapolation to zero stress should eliminate the contribution of plastic or viscous flow.

This simple concept was worked out in practice by measuring peel velocity against peel angle for different peel forces and temperatures. Peel velocity, $\dot{c}$, was extrapolated to zero to give a critical angle of peel, ϕ_c for a given peel force and temperature, and Equation 2 used to abstract an apparent (app) θ_0 value. This value increased with both load and temperature and therefore cannot be a true θ_0. However, if this quantity, θ_0(app), is plotted against load, the resulting linear plot extrapolates at zero load to a value which is independent of temperature. This extrapolated value is taken as the true θ_0, and this assumption will be discussed at the end of the paper.

3. Materials

A single adhesive was used throughout this study, being a proprietary surgical adhesive supplied by Smith and Nephew Research Ltd. Gilston Park, Harlow, Essex. The adhesive was a natural-rubber based material conforming to BP specification and containing natural rubber, colophony resin, lanolin and zinc oxide. Specimens were prepared by spreading the adhesive from solvent on to a backing of woven cotton in such a way that the warp threads lay in the pulling direction during peel testing. This ensured that no significant extension of the peel strip occurs in testing and thus permits the use of Equation 2 in analysing the data.

The most detailed work was carried out using soda glass as a substrate. The second substrate employed was human skin, namely the inner aspect of the forearm of a volunteer. This measurement was, of course, essential to the purpose of this study, since we wished to compare θ_0 values for living human skin and for the glass reference surface. Clearly, however, the time required for detailed measurements was not tolerable for *in vivo* determinations (glass measurements often ran overnight, for example). Nor was it possible to vary temperature in the *in vivo* experiments because of the thermostatic effect of the skin. The results of the *in vivo* tests do not therefore have the accuracy obtained with glass substrates, but are found to be wholly consistent with the more detailed work as we shall see.

4. Experimental details

4.1. Preparation of adhesive strips

The adhesive, diluted with petroleum spirit was spread over woven cotton cloth held flat on release paper, forming a band 10 cm wide. Some of the solution penetrated the sheet. The petroleum spirit was allowed to evaporate for 24 h and a second sheet of release paper placed over the rubber. Thus a cotton-reinforced adhesive sheet was produced, protected on both sides by release paper. The average weight of adhesive was 330 gm^{-2} the weight of cotton being an additional 90 gm^{-2}. For testing, 140 × 10 mm strips were cut from the sheet.

4.2. Preparation of test samples

Soda glass slides, 150 × 20 mm, were cleaned with acetone by soaking and swabbing, given a final rinse and allowed to drain. The originally upper surface of the adhesive strips, after removal of the release paper, was applied to the glass, leaving a short tab at one end separated from the glass with tissue to facilitate subsequent peeling. Obvious discontinuities of contact between glass and rubber were removed by rubbing the release paper on the back of the strip with a round-tipped rod. This release paper was removed immediately before testing.

4.3. Apparatus and test procedure

The apparatus for peeling from glass consisted essentially of a slotted platform which could be tilted to provide angles of peel (ϕ) between 30 and 150°. The glass slides were fastened across the slot, leaving the peel strip free to peel through the slot. A weight was suspended from the tab by means of a clip and a black cotton thread. Fig. 1 illustrates the arrangement.

As the strip peeled, the cotton suspension thread moved past a double 1 cm grid of vertical black cotton threads placed behind the rig. The alignment of the suspension cotton with successive pairs of cottons of the grid could thus be timed, the double grid ensuring the absence of parallax errors. The rate of peel was calculated for each interval.

The whole rig was mounted in a glass-fronted chamber fitted with cooling and heating coils. The temperature was measured by thermometers placed each side of the rig and was noted at intervals during the test (constancy within ±0.5° C was generally achieved). In long tests the weight was removed overnight and replaced the next day with no discontinuity in rate or mode of peeling being observed.

4.4. Test conditions

Temperatures of 10, 19, 32 and 35° C were used and

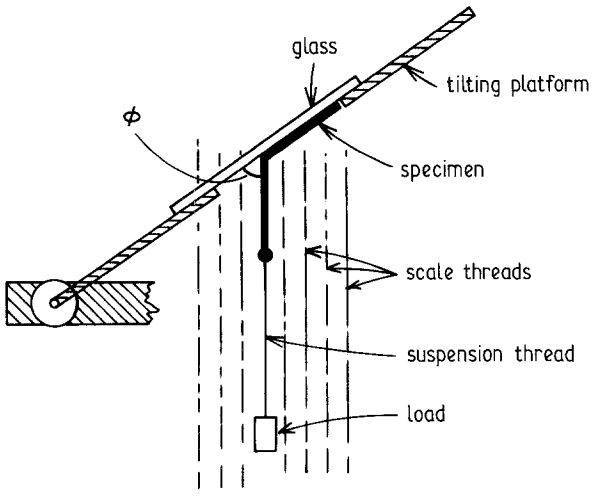

Figure 1 Dead-load peel testing at variable peel angle ϕ.

weights of P = 110, 160, 225 and 275 g (including the weight of the clip). On a 10 mm wide strip these loads correspond to forces per unit width, F = 108, 157, 221 and 270 Nm^{-1} respectively. Angles of peel, ϕ, were varied from 45 to 135°, the particular range employed varying with the other test conditions. Note that $F = P/b$ where b is the peel-strip width.

4.5. Examination after testing

The position of the final crack-front and the unpeeled end of the strip were marked on the glass as datum points. The strip was removed and a scale diagram prepared showing modes of failure (adhesive or cohesive), the amount of rubber adhering to the glass for cohesive regions and other features which seemed of interest. The adhesive strip was then cut into 5 to 15 mm lengths, corresponding to different rates or modes of peeling, and weighed. Substantial amounts of rubber attached to the glass were removed and their weights determined. Thus local weights of adhesive, temperature and other observations made during the run could be correlated with rates and modes of peeling.

4.6. Peeling from skin

The peel strips were identical to those used on glass substrates but were applied to the inner aspect of the forearm of a single volunteer. The forearm was supported on a simple wooden ramp whose inclination to the vertical could be set at any angle from 0 to 90°. The ramp was slotted down the middle to allow the peel strip to be peeled under a dead load.

Peeling speed was measured by marking the peel strip at 1 cm intervals and timing appropriately as a function of load and peel angle. It should be noticed that the skin is "plucked up" by the peel strip so that the angle between the skin and the adhesive strip at the point of separation is always larger than the peel angle ϕ. However, this does not affect the mechanics of the process and Equation 2 is still applicable, since the ratio of load displacement to peeled length is determined uniquely by ϕ, not the *local* angle between peel strip and substrate.

Data were generated for peel velocity versus angle for four different loads. The skin temperature was also measured by contact thermocouple.

5. Results

5.1. Corrections to observed rates

The peeling rates were corrected or normalized as follows:

1. If the width of the strip differed by more than 2% from the nominal 10 mm, an adjustment was made on the assumption that for small errors the rate would be inversely proportional to the width.

2. A temperature correction was made for each rate determination if the temperature varied from its nominal value by more than 0.5° C. This could only be done in retrospect, when enough tests had been made to establish approximate temperature coefficients.

3. For each test, adhesive and cohesive peel rates ($\dot{c}_A$, $\dot{c}_c$) were plotted against weight per unit area of adhesive. A reasonably smooth curve could usually be drawn from which the peel rates for selected adhesive weights could be found by interpolation. Examples of such curves are shown in Fig. 2. As the weight (i.e. thickness) of the adhesive increases, $\dot{c}_A$ decreases, eventually to less than the relatively invarient $\dot{c}_c$. Where the cohesive mode predominates, adhesive rates can be estimated by a limited extrapolation. Among other features, curves in Fig. 2 illustrate good reproducibility between samples (Fig. 2b); transitions from adhesive to cohesive mode as the thickness and peel angle increases (Fig. 2c); and that for very thick samples $\dot{c}_c$ may show a slight increase with increasing weight (Fig. 2d).

5.2. Variation of peel rate with peel angle

5.2.1. Tests at 10° C

Fig. 3 is an example of $\dot{c}_A$ plotted against ϕ, for F = 221 Nm^{-1}, and the standard weight of adhesive, 33 $mg\,cm^{-2}$. The same data are plotted on an expanded scale for the lower values of ϕ, in Fig. 4, with the addition of $\dot{c}_A$ for lower adhesive weights and $\dot{c}_c$.

At low values of ϕ ($<45°$) cohesive peeling (filled symbols) is faster, than adhesive peeling (open symbols) but with increasing ϕ, $\dot{c}_c$ changes little, while $\dot{c}_A$ increases slowly. Adhesive peeling is first observed for lower adhesive weights. Around $\phi \sim 65°$, $\dot{c}_A$ begins to increase more quickly, and the plot becomes nearly linear. Cohesive peeling is not usually observed under these conditions, but at very high values of ϕ, $\dot{c}_A$ may decrease and cohesive peeling re-appear.

The curves for F = 270 and 157 Nm^{-1} are similar in character to Figs 3 and 4 provided the rate scales are suitably chosen. The cohesive failure mode is more often observed with the lower values of F, and for F = 108 Nm^{-1}, the mode is cohesive up to ϕ = 65°.

5.2.2. Tests at 19° C

The curves resemble those for 10° C, peeling being 6 to 10 times faster.

5.2.3. Tests at 32 and 35° C

The rubber flows, to form filaments, much more readily at these temperatures and the cohesive mode of peeling may be observed over the whole range of ϕ, even where the adhesive rate is faster. The build-up of massed long filaments tends to slow the rate, inducing

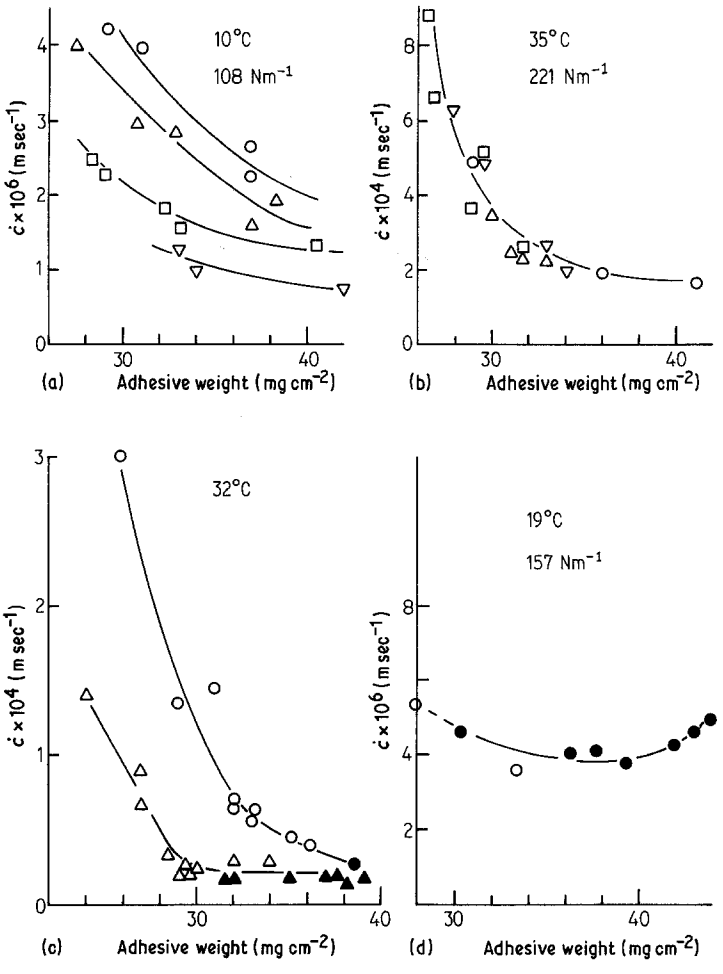

Figure 2 Effect of adhesive loading (thickness) on peel velocity $\dot{c}$, for various peeling angles. Values given are temperature in °C and peel force per unit width of tape (Nm^{-1}). (a) Smooth dependence on adhesive loading. Peeling angles: (▽) 90°, (□) 103°, (△) 119°, (○) 127°. (b) Good reproducibility between different samples (different symbols) at a peeling angle of 90°. (c) Transition from adhesive (open symbols) to cohesive (closed symbols) as thickness increases and $\dot{c}$ decreases. (○) 221 Nm^{-1}, 68.5°, (△) 108 Nm^{-1}, 98.5°. (d) Rise in $\dot{c}_c$ at high loadings, at a peel angle of 55°. (●) cohesive (○) adhesive.

and tending to maintain the cohesive mode. A set of curves for $F = 157\,Nm^{-1}$ at 32° C is shown on Fig. 5.

Unlike the 10 and 19° C data, there is a steady increase in $\dot{c}_c$ with increasing ϕ. At $\phi > 132°$, no adhesive peeling was observed at the higher temperatures.

At lower values of F, and at 35° C, the trend to cohesive peeling is more common, but there were sufficient adhesive results to obtain curves.

5.3. Extrapolation to zero adhesive peeling rate

In Figs 3 to 5, the curves have been extrapolated by hand to the ϕ-axis, in order to obtain a value for the angle ϕ_c at which $\dot{c}_A$ becomes zero. Although $\dot{c}_A$ varies with adhesive weight (and sometimes with the batch of test-pieces), the curves all extrapolate to the same

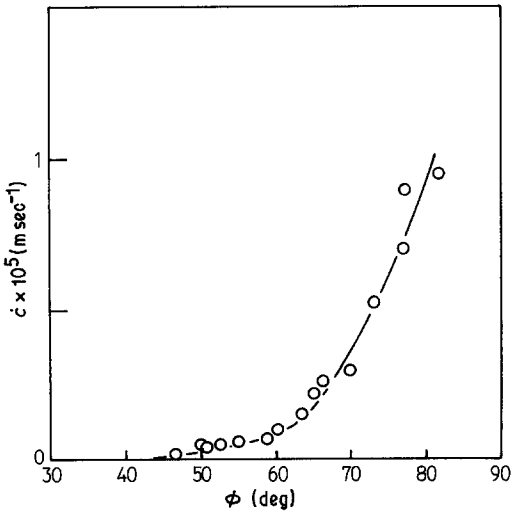

Figure 3 Peel velocity $\dot{c}$ as a function of peel angle ϕ: at 10° C and 221 Nm^{-1} force per unit width.

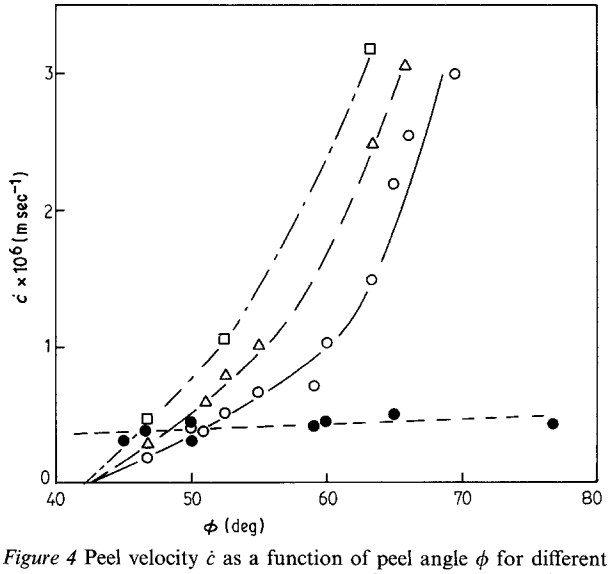

Figure 4 Peel velocity $\dot{c}$ as a function of peel angle ϕ for different loadings of adhesive (□) 28 mg cm^{-2}, (△) 30 mg cm^{-2}, (○) 33 mg cm^{-2}, (●) cohesive. The cohesive characteristic is also shown (filled symbols).

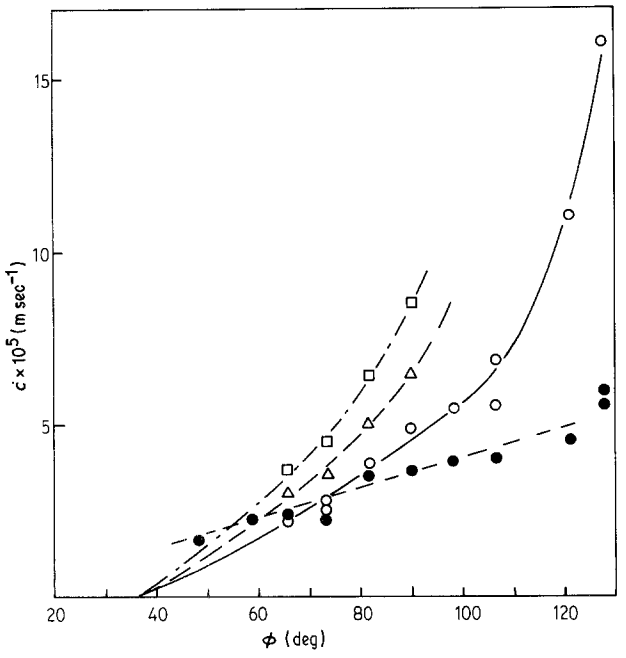

Figure 5 Peel velocity $\dot{c}$ as a function of peel angle ϕ at 32° C and 157 Nm^{-1}. (□) 28 mg cm^{-2}, (△) 30 mg cm^{-2}, (○) 33 mg cm^{-2}, (●) cohesive.

value of ϕ_c, and this is true for all test conditions examined. However, the curved extrapolation is not easy, and there is a large margin of error, particularly since cohesive data tend to predominate at low peel angle. An alternative method was therefore sought to obtain the critical angle (and thence ϕ_0 (app)).

5.4. Alternative procedure for ϕ_0

In order to reduce the number of steps to the final estimation of ϕ_0, the rate of peeling can be plotted against $F(1 - \cos \phi)$, the extrapolation to zero rate then giving $F(1 - \cos \phi_c)$ or θ_0(app) directly. An advantage of this procedure is that the important low-ϕ points lie on straight lines, or nearly so. The results of the tests at 19° C are plotted, by way of example, in Figs 6 to 9. Two intersecting straight lines represent each condition of test, meeting at points corresponding to the bends in the rate against ϕ curves.

The lower of these intersecting lines have been

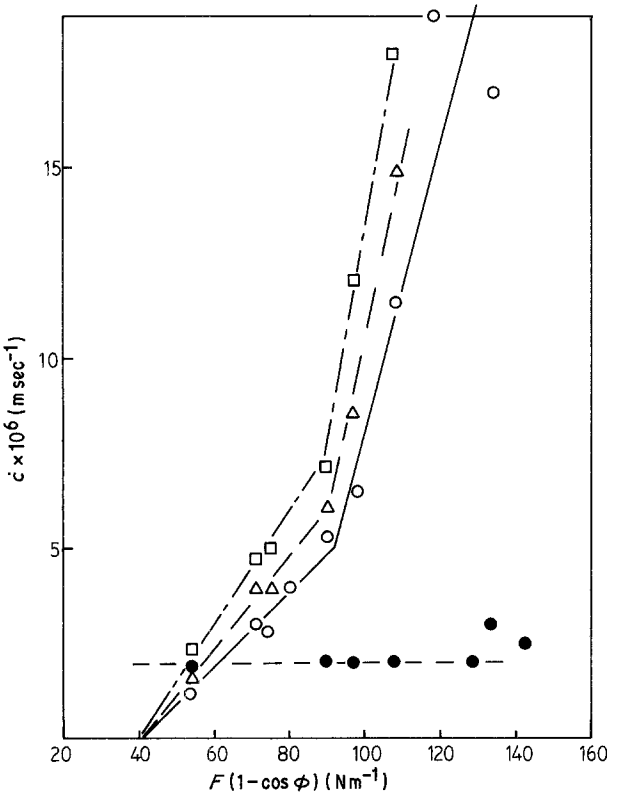

Figure 6 Peel velocity $\dot{c}$ as a function of the parameter $F(1 - \cos \phi)$ for different adhesive loadings at 19° C and F = 108 Nm^{-1}. (□) 28 mg cm^{-2}, (△) 30 mg cm^{-2}, (○) 33 mg cm^{-2}, (●) cohesive.

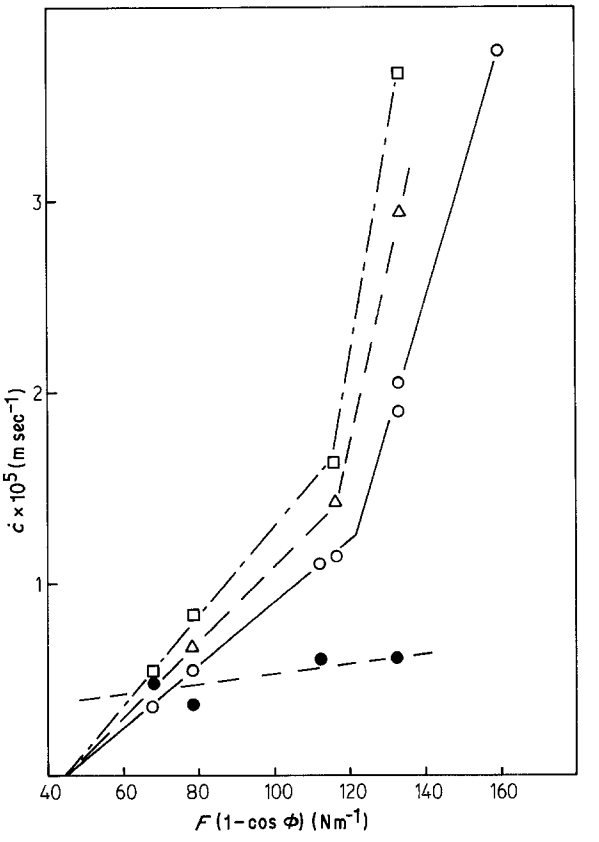

Figure 7 Peel velocity $\dot{c}$ as a function of the paramter $F(1 - \cos \phi)$ for different adhesive loadings at F = 157 Nm^{-1}, 19° C. (□) 28 mg cm^{-2}, (△) 30 mg cm^{-2}, (○) 33 mg cm^{-2}, (●) cohesive.

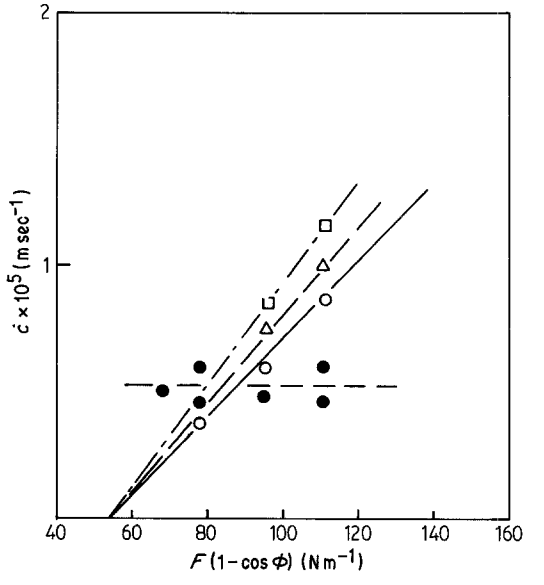

Figure 8 Peel velocity $\dot{c}$ as a function of the parameter $F(1 - \cos \phi)$ for different adhesive loadings at F = 221 Nm^{-1}, 19° C. (□) 28 mg cm^{-2}, (△) 30 mg cm^{-2}, (○) 33 mg cm^{-2}, (●) cohesive.

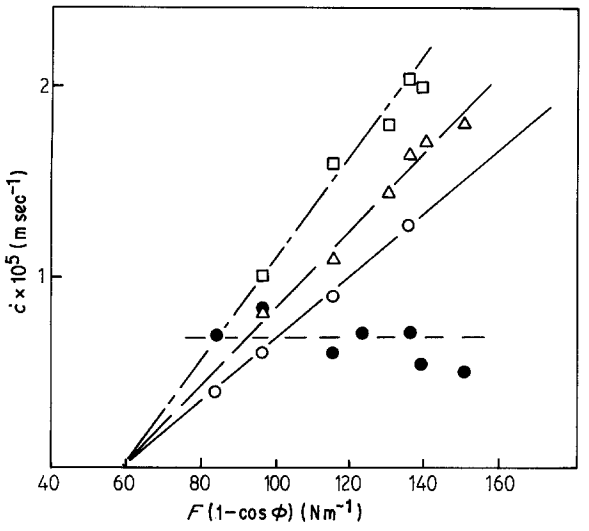

Figure 9 Peel velocity $\dot{c}$ as a function of the parameter $F(1 - \cos \phi)$ for different adhesive loadings at $F = 270\,\mathrm{Nm^{-1}}$, 19° C. (□) 28 mg cm^{-2}, (△) 30 mg cm^{-2}, (○) 33 mg cm^{-2}, (●) cohesive.

extrapolated to zero rate, and the values of $F(1 - \cos \phi_c)$ so obtained are plotted against F for the four temperatures of test in Figs 10 to 13. The range of values is indicated for each point, the circle being considered the most probable value. The broken "error bars" show the usually greater range deduced from the less accurate extrapolations of rate against ϕ plots.

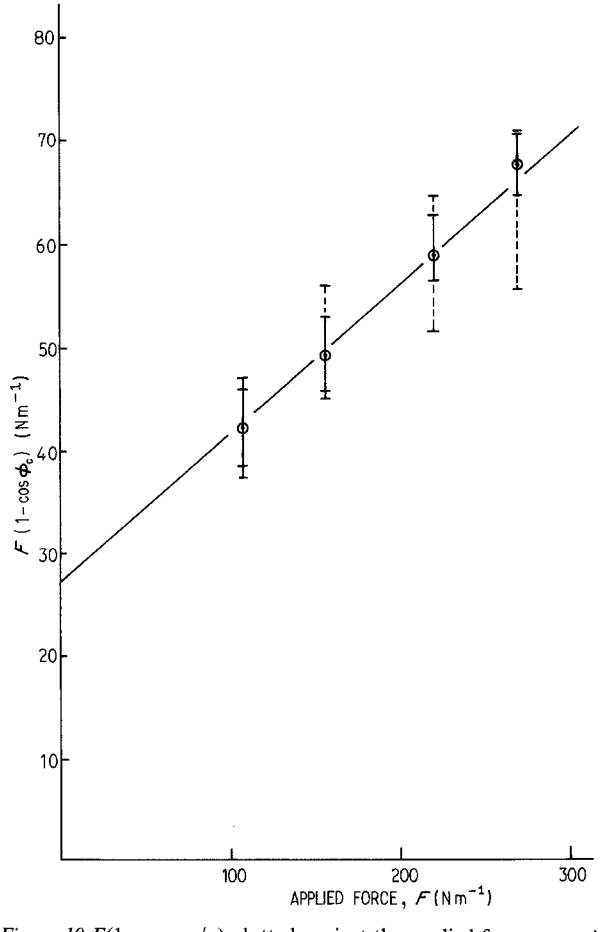

Figure 10 $F(1 - \cos \phi_c)$ plotted against the applied force per unit width. ϕ_c is the critical angle for crack arrest. Line extrapolated to zero force gives true θ_0. Data for 10° C.

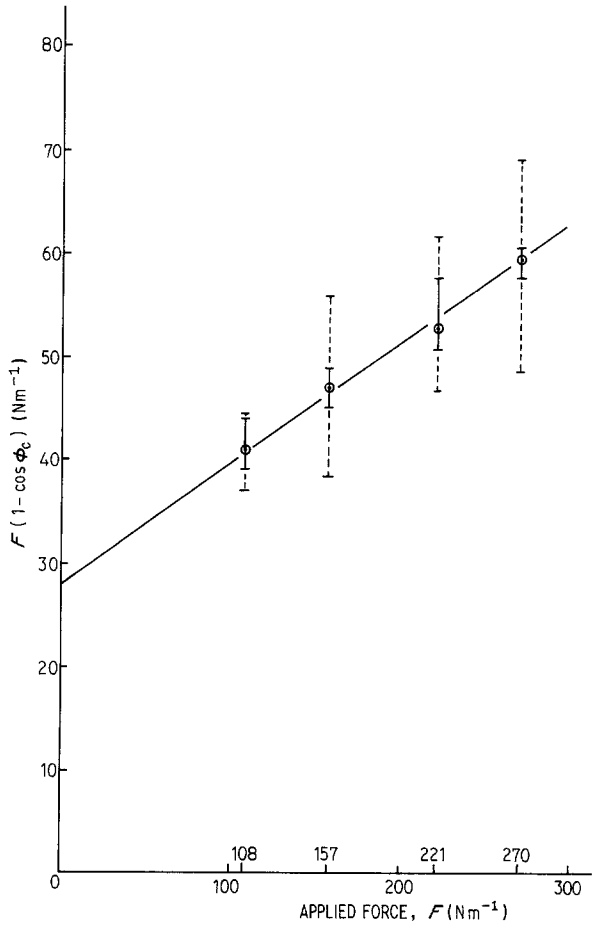

Figure 11 $F(1 - \cos \phi_c)$ plotted against the applied force per unit width. ϕ_c is the critical angle for crack arrest. Line extrapolated to zero force gives true θ_0. Data for 19° C.

In Fig. 14, the final results for all four temperatures (without error bars), are put together, and clearly extrapolate to the same value independent of temperature. This value is, $\theta_0 = 28.0 \pm 1.0\,\mathrm{J\,m^{-2}}$, for the natural-rubber based adhesive and soda glass. It is also of note that the slopes of the lines in Fig. 14 increase systematically as the temperature falls.

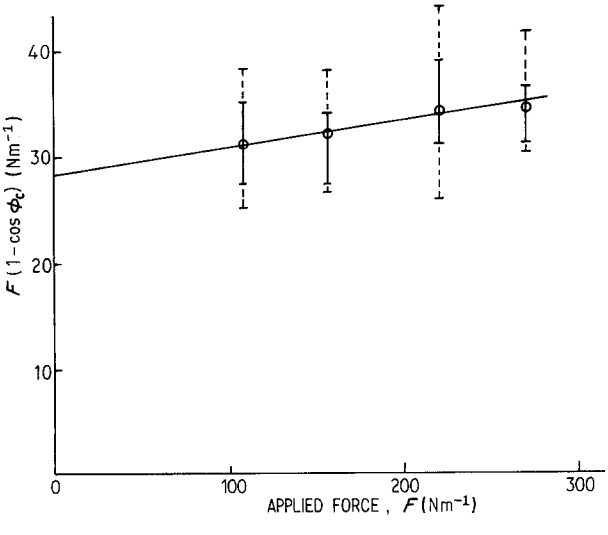

Figure 12 $F(1 - \cos \phi_c)$ plotted against the applied force per unit width. ϕ_c is the critical angle for crack arrest. Line extrapolated to zero force gives true θ_0. Data for 35° C.

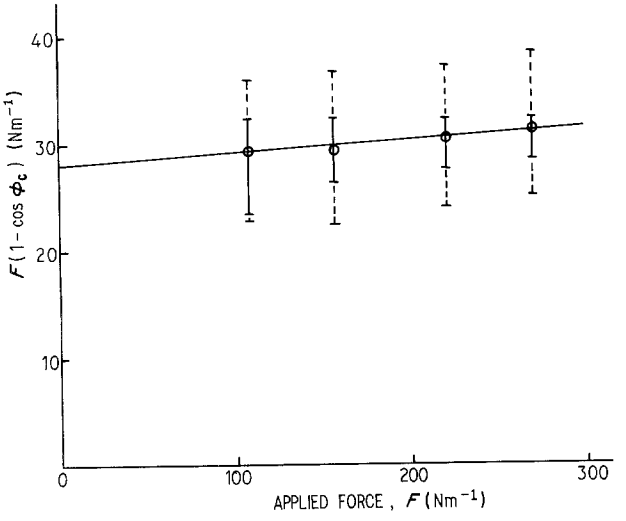

Figure 13 $F(1 - \cos \phi_c)$ plotted against the applied force per unit width. ϕ_c is the critical angle for crack arrest. Line extrapolated to zero force gives the true θ_0. Data for 35° C.

5.5. Data for skin

Following the analysis used for glass substrates, the data for skin have been plotted as velocity against $F(1 - \cos \phi)$ and examples at low and high load are given in Fig. 15. Linear extrapolations can be made to provide the critical parameter $F(1 - \cos \phi_c)$ for a given load.

A new complication arises, however, at the higher loads. As the peeling angle decreases towards 30° the peeling velocity begins to rise again, against all expectations from theory and the evidence with glass substrates. This unexpected result is quite easy to explain in terms of the energy of deformation of the skin. *In vivo*, the substrate is itself deformable and can store energy when loaded, which is then released as peeling proceeds. This energy release becomes non-zero as soon as the deformed zone in the skin exceeds the length of the bonded peel strip. It rapidly becomes large relative to the potential energy loss of the falling weight as $\phi \to 0$ (just as the elastic stored energy in the peeled portion of the strip becomes important at low ϕ unless the strip is very stiff in tension, Kendall [12]). The velocity therefore rises again as $\phi \to 0$.

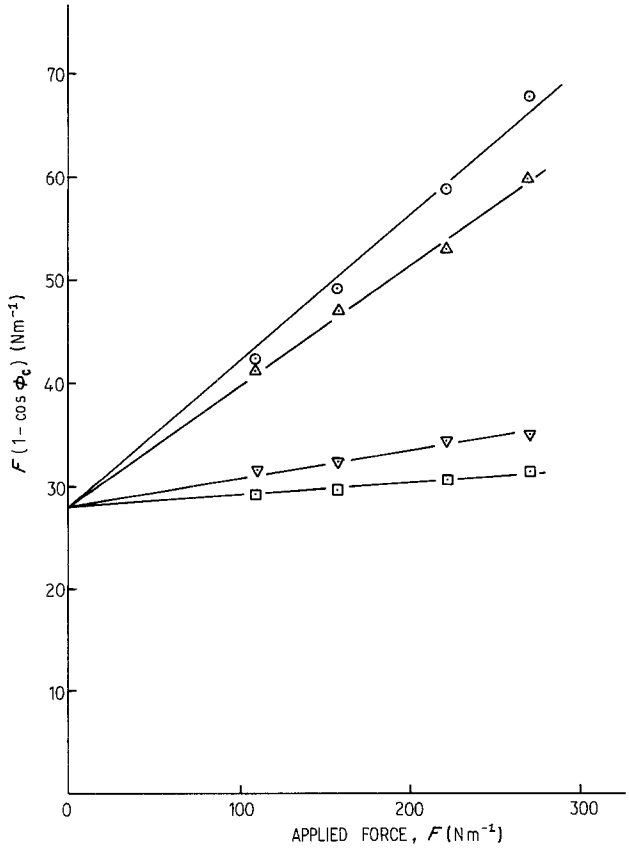

Figure 14 $F(1 - \cos \phi_c)$ or θ_0(app), for glass substrates against applied force per unit width, showing temperature independent intercept at $F = 0$. (⊙) 10° C, (△) 19° C, (▽) 32° C, (□) 35° C.

These effects, although they increase the difficulty of extrapolating accurately, do not invalidate the extrapolation of high ϕ data to zero velocity. This is because there is no net energy release from the skin as long as the deformed region of the skin does not extend the whole length of the adhering strip. Until it does, peeling only propagates a constant-volume zone of deformation in the skin along the forearm, dissipating energy but creating no net energy release to help drive the debonding process.

Finally, therefore, the apparent θ_0 is obtained, as before, from

$$\theta_0(\text{app}) = F(1 - \cos \phi_c)$$

and the resulting values are plotted against F in Fig. 16. Because of the limited data and large scatter arising from the problems of an *in vivo* test, it is not easy to define a linear relationship analogous to those obtained with glass as the substrate. However, the "glass data" come to our assistance by indicating the slope to be expected, namely that for a temperature of 32° C, the measured skin temperature. Assuming that this slope depends only on temperature and not on substrate, we may thus construct the line shown in Fig. 16, having the required slope and being consistent with the error bars on θ_0(app). This leads to the conclusion that, for skin, θ_0(true) = $14 \pm 3\,\text{J m}^{-2}$. This compares with a value of $28\,\text{J m}^{-2}$ for glass substrates. Of course, θ_0 for skin will depend upon moisture transpiration and other physiological factors, and should therefore be regarded as a typical, rather than an absolute value. It will fall dramatically in the presence of perspiration, as discussed elsewhere [13].

6. Discussion

The first question to consider is the validity of the θ_0 figure for glass substrates. Our value may be compared with the results of Ahagon and Gent [10] who carried out low-rate peeling tests on crosslinked rubber and noted the point at which peeling energy became rate independent (see Table I).

TABLE I θ_0 values in J m^{-2}

Adhesive	Crosslinking	Substrate	θ_0	Source
NR surgical	None	glass	28	*
Polybutadiene	Low†	glass	~50	[10]
Polybutadiene	High‡	glass	10	[10]
Polybutadiene	Low†	ethyl silane treated glass	3	[10]
Polybutadiene	High‡	ethyl silane treated glass	1.5	[10]

*This work.
†Using 0.05% dicumyl peroxide for crosslinking.
‡Using 0.2% dicumyl peroxide.

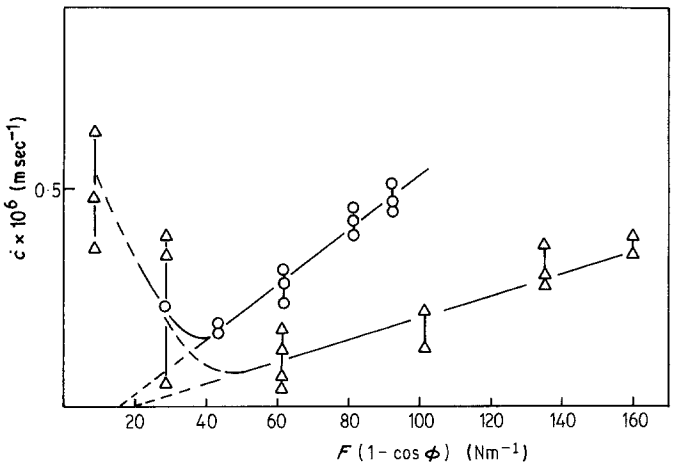

Figure 15 Peel velocity $\dot{c}$ as a function of the parameter $F(1 - \cos\phi)$ for skin substrates for two different applied loads. Note upturn in curve at small $F(1 - \cos\phi)$. (○) 56 Nm^{-1}, (△) 216 Nm^{-1}.

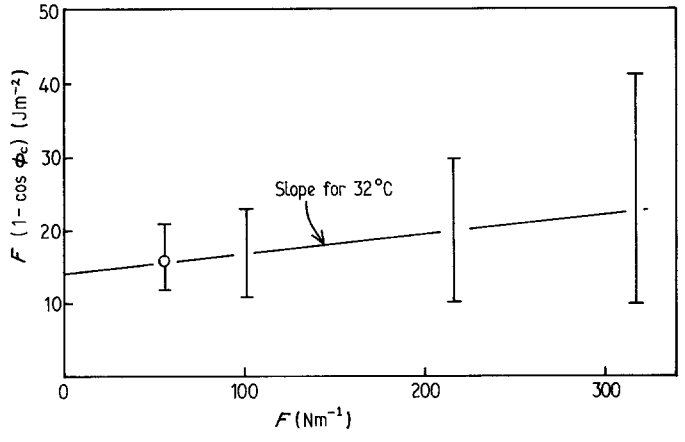

Figure 16 $F(1 - \cos\phi_c)$, or θ_0(app), for skin substrate against applied force per unit width.

Our results for uncrosslinked natural rubber compare well with the figure obtained by Ahagon and Gent for low degrees of crosslinking especially when it is remembered that our surgical adhesive contains only about 50% by weight of polymer. Table I also shows that higher degrees of crosslinking decrease θ_0 as does a reduction in surface energy of the glass by treating with ethyl silane (which unlike vinyl silane cannot form chemical bonds with the elastomer).

Ahagon and Gent discussed the fact that θ_0 for rubberlike adhesives far exceeds the values to be expected for thermodynamic works of adhesion ($w_A \sim 0.5\,J\,m^{-2}$ for clean glass, $0.05\,J\,m^{-2}$ for silane treated glass). They attributed this result to the Lake–Thomas effect [14], namely that in a crosslinked molecular network, all the C–C bonds in a network chain must be energised to breaking point before one fails. The energy required to break the network chain is therefore a multiple of that required to break one bond.

We conclude therefore that the θ_0 value of $28\,J\,m^{-2}$ determined for a surgical adhesive and a glass substrate is consistent with previous data on lightly crosslinked adhesives. This in turn vindicates the "double extrapolation" method employed (i.e. extrapolation both to zero velocity and zero load).

Turning to the θ_0 result for skin, we see that this is typically lower than for glass, by a factor of about two. This figure applies to "dry" skin, that is below the environmental temperature at which liquid perspiration takes place.

In work to be reported in detail elsewhere [13] but shown in Fig. 17, it was found that the total work of peeling, θ, for the same natural rubber surgical adhesive, was about equal for skin and glass substrates at 37° C (body temperature). This means that in the

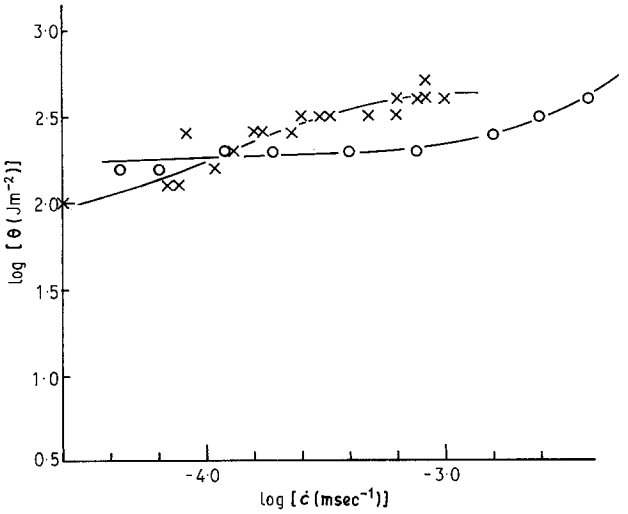

Figure 17 Total peeling energy θ for glass and skin substrates at 37° C as a function of the peel velocity. (×) glass, (○) skin.

TABLE II Values of Φ at 37° C

Substrate	Peeling rate (ms^{-1})		
	10^{-5}	10^{-4}	10^{-3}
Skin	13	14	16
Glass	2–3	7	14

equation

$$\theta = \theta_0 \Phi \quad (1)$$

the loss-function Φ with skin as the substrate is about twice the value for a glass substrate. Thus the energy dissipation in the skin is similar to that in the adhesive during peeling. The actual values of Φ vary, of course, with rate and temperature, but at 37° C the values are as given in Table II. This shows that energy dissipation in the skin dominates at low rates but reduced both relatively and absolutely as the peeling speed increases to 1 mm sec^{-1}.

Acknowledgements

The authors are grateful to SERC for a research support grant and to Smith and Nephew Research Ltd. for the supply of adhesive and for helpful discussion.

References

1. E. H. ANDREWS, T. A. KHAN and H. A. MAJID, *J. Mater. Sci.* **20** (1985) 3621.
2. E. H. ANDREWS, T. A. KHAN, J. K. RIEKE and J. F. RUDD, *J. Clinic. Mater.* **1** (1986) 205.
3. A. N. GENT and J. SCHULTZ, *J. Adhesion* **3** (1972) 281.
4. E. H. ANDREWS and A. J. KINLOCH, *Proc. R. Soc.* **A332** (1973) 385.
5. *Idem, J. Polym. Sci. Sympos.* **46** (1974) 1.
6. E. H. ANDREWS, *J. Mater. Sci.* **9** (1974) 887.
7. E. H. ANDREWS and N. E. KING, *ibid.* **11** (1976) 2004.
8. A. STEVENSON and E. H. ANDREWS, in "Adhesion 3", edited by K. W. Allen (Appl. Science Publishers, Barking, 1979) p. 81.
9. E. H. ANDREWS, HE PINGSHENG and C. VLACHOS, *Proc. R. Soc.* **A381** (1982) 345.
10. A. AHAGON and A. N. GENT, *J. Polym., Sci. Polym. Phys. Ed.* **13** (1975) 1285.
11. K. KENDALL, *J. Adhesion* **7** (1974) 55.
12. *Idem, J. Phys. D. Appl. Phys.* **8** (1975) 1449.
13. T. A. KHAN and E. H. ANDREWS (to be published).
14. G. J. LAKE and A. G. THOMAS, *Proc. R. Soc.* **A300** (1967) 108.

Received 11 September
and accepted 8 December 1986